Proceedings of the 8th International Conference on Gas Hydrates (ICGH8-2014),
Beijing, China, 28 July - 1 August, 2014

REVIEW OF THE FINDINGS OF THE IĠNIK SIKUMI CO_2-CH_4 GAS HYDRATE EXCHANGE FIELD TRIAL

Brian ANDERSON*
Department of Chemical Engineering, West Virginia University and National Energy Technology Laboratory, Morgantown WV 26507, USA

Ray BOSWELL
National Energy Technology Laboratory, Pittsburgh PA 15236, USA

Timothy S. COLLETT
U.S. Geological Survey, Denver CO 80225, USA

Helen FARRELL
ConocoPhillips, Houston TX 77252, USA

Satoshi OHTSUKI
Japan Oil, Gas and Metals National Corporation, Chiba JAPAN

Mark WHITE
Pacific Northwest National Laboratory, Richland WA, 99352, USA

Margarita ZYRIANOVA
U.S. Geological Survey, Denver CO 80225, USA

ABSTRACT

The Iġnik Sikumi Gas Hydrate Exchange Field Trial was conducted by ConocoPhillips in partnership with the U.S. Department of Energy, the Japan Oil, Gas, and Metals National Corporation, and the U.S. Geological Survey within the Prudhoe Bay Unit on the Alaska North Slope (ANS) during 2011 and 2012. The 2011 field program included drilling the vertical test well and performing extensive wireline logging through a thick section of gas-hydrate-bearing sand reservoirs that provided substantial new insight into the nature of ANS gas hydrate occurrences. The 2012 field program involved an extended, scientific field trial conducted within a single vertical well ("huff-and-puff" design) through three primary operational phases: 1) injection of a gaseous phase mixture of CO_2, N_2, and chemical tracers; 2) flowback conducted at down-hole pressures above the stability threshold for native CH_4-hydrate, and 3) extended (30-days) flowback at pressures below the stability threshold of native CH_4-hydrate. Iġnik Sikumi represents the first field investigation of gas hydrate response to chemical injection, and the longest-duration field reservoir response experiment yet conducted. Full descriptions of the operations and data collected have been fully reported by ConocoPhillips and are available to the science community. The 2011 field program indicated the presence of free water within the gas hydrate reservoir, a finding with significant implications to the design of the exchange trial – most notably the requirement to use a mixed gas injectant. While the use of mixed gas, as opposed to pure CO_2, resulted in a complex chemical environment within the reservoir that greatly tests current experimental and modeling capabilities – without such a mixture, it is apparent that injection could not have been achieved. Although interpretation of the field data is continuing, the primary scientific findings and implications recognized to date are: 1) gas hydrate destabilization is self-limiting, dispelling any notion of the potential for uncontrolled destabilization; 2) wells must be

* Corresponding author: Phone: 304-293-9334 Fax 304-293-4139 E-mail: brian.anderson@mail.wvu.edu

carefully designed to enable rapid remediation of wellbore blockages that will occur during any cessation in operations; 3) appropriate gas mixes can be successfully injected into hydrate-bearing reservoirs; 4) sand production can be well-managed through standard engineering controls; 5) reservoir heat exchange during depressurization was much more favorable than expected – mitigating concerns for near-well-bore freezing and enabling consideration of more aggressive pressure reduction and; 6) CO_2-CH_4 exchange can be accomplished in natural reservoirs, although the extent is not yet known. The next steps in evaluation of exchange technology should feature multiple well applications; however such field programs will require extensive preparatory experimental and numerical modeling studies and will likely be a secondary priority to further field testing of production through depressurization.

Keywords: gas hydrates, exchange, CO_2, Alaska

NOMENCLATURE

S_w, S_g, S_{gh},	Saturation of water (*w*), gas (*g*), and gas hydrate (*gh*)
s_{gr}, s_{lr}	Irreducible gas and liquid saturations
R_t	Formation (*t*) or water (*w*) resistivity
a,*m*	Archie's constants
k	Permeability, mD
k_{eff}	Effective permeability
φ	Porosity

INTRODUCTION

Research into the practical applications of CO_2-CH_4 exchange in hydrates has been conducted in laboratories and via numerical simulation since the mid-1990s. Initial studies, which commonly used pure CO_2 and bulk hydrates with no water present, documented the chemical basis for exchange (Goel, 2006). However, the observed low-rate kinetics of the exchange reaction rendered the process a less attractive option for gas hydrate production as compared to depressurization, which showed increasingly positive results in laboratory, experimental, and field applications (Moridis et al., 2009) .

Interest in CO_2-CH_4 exchange was re-kindled in the 2000s based upon promising results from experimental and numerical modeling efforts at PNNL (McGrail et al., 2007). A collaborative R&D effort between the U. Bergen and ConocoPhillips (Graue, 2008; Baldwin et al., 2009; Hester et al., 2011) conducted within a porous media context and at P/T conditions that closely mimicked known Alaska North Slope gas hydrate occurrences indicated 1) relatively rapid CH_4 release (as much as 50% of the rate observed for depressurization in similar samples); 2) exchange of CH_4 with CO_2 at roughly the theoretical limit (approaching 70%); and 3) no observation of significant water-liberated at any time during the process (Stevens et al., 2008). However, these initial experiments utilized samples in which pore space was filled with gas hydrate and free gas (no free water present). As emerging field data indicated that free water was a likely common constituent of gas hydrate occurrences in nature (Collett et al., 2009), attempts to recreate these experimental findings using samples that include free water were attempted. These studies proved to be extremely challenging and produced inclusive results, and as a result, it was determined that the next step in the evaluation of the technology was to conduct a controlled scientific experiment in a field setting. Following an extensive review of potential field opportunities, the location selected was the vicinity of the Prudhoe Bay Unit L-pad on the Alaska North Slope, (Schoderbek et al., 2013).

On May 5, 2012, ConocoPhillips, in a cooperative R&D effort with the Japan Oil, Gas, and Metals National Corporation and the U.S. Department of Energy, completed the first field program designed to investigate the potential for CO_2-CH_4 exchange in naturally-occurring methane hydrate reservoirs from a temporary ice pad constructed in the Prudhoe Bay Unit on the Alaska North Slope. The purpose of this report is to provide initial scientific interpretation of the logging and field testing data, to describe further work remaining, and to indicate initial lessons-learned regarding the potential of gas hydrate production via CO_2-CH_4 exchange. For further background and information on the Iġnik Sikumi project and the operational details of the field trial, please see Schoderbek et al. (2013).

The Iġnik Sikumi field program consisted of 1) well drilling and logging phase (2011), 2) temporary well abandonment over the Spring-Summer, and Fall of 2011, 3) gas injection and

production during early 2012, and 4) final well abandonment and site remediation.

The primary objectives of the 2011 field program were install a fully-instrumented completion suitable for conducting the field trail and to gather additional field data to 1) more fully characterize the occurrence and nature of gas hydrates at the site as well as to improve the understanding of gas hydrate occurrence within the greater Prudhoe Bay region; and 2) enable the final design of the subsequent field trial. Among the primary information gathered in 2011 (summarized in greater detail in "2011 Logging Results" below) was the confirmation of the co-occurrence of concentrated gas hydrate (up to 80% of pore volume), bound water (up to 10% of pore volume) and free (mobile and reactive) water (up to 10% of pore volume) in units with high intrinsic reservoir quality.

The primary objectives of the 2012 field program was to demonstrate the ability to inject gas mixes into a gas-hydrate-/free-water-bearing reservoir, and to produce the reservoir via a staged approach of pressure reduction that would provide the best opportunity to interpret the nature of reservoir response to both the injection and the succeeding depressurization. To achieve these goals, the injectant used was a mixture of CO_2 (23%) and N_2 gas (77%) with minor amounts of chemical tracers. This mixture was designed based on recognition that the formation would contain significant quantities of free water that would effectively block the injection of pure CO_2.

The Iġnik Sikumi field trail was conducted as a "huff and puff" within a single vertical well. While this design is not an optimal design for potential commercial application of exchange technology (which would likely include multiple deviated wells with separate injectors and producers), it is in accord with the operational constraints (single season operation from a temporary ice-pad) and scientific objectives of the of an initial field program.

The trial proceeded through the following stages 1) injection (14 days), 2) soak (X days); 3) unassisted flow-back (1.5 days), and 4) jet-pump-assisted flow-back (30 days). This fourth stage was accomplished via three phases: 1) production at pressures above the destabilization pressure of both native CH_4 hydrate and any complex hydrate formed during the injection phase (~9 days); 2) production at conditions in close proximity to the native CH_4-hydate stability (~2.5 days); and 3) production via depressurization at pressures below native CH_4-hydrate stability (~18.5 days).

2011 FIELD PROGRAM RESULTS

Logging Results

The 2011 Iġnik Sikumi field program included the acquisition of mud logging data, logging-while-drilling (LWD) the 13½" "top hole" and the 9⅞" "production test" portion of the well, and a comprehensive open-hole wireline logging suite in the 9⅞" "production test" portion of the well, including the deployment of the Platform Express (PEX), Combinable Magnetic Resonance (CMR), Pressure Express (XPT), and Modular Dynamic Tool (MDT).

Log responses for the gas hydrate reservoir interval (Schoderbek et al., 2012, 2013) indicate generally good quality borehole conditions throughout the hydrate-bearing units with minimal washout (Figure 1). The hydrate-bearing intervals are identified by relatively high resistivity and low compressional-wave acoustic slowness log values. The presence of gas hydrate can also be inferred by the separation between the conventional density and CMR (also known as nuclear magnetic resonance, NMR, log data) porosity curves. The gamma-ray log indicates that the well-log-inferred gas hydrates occur in sand-rich intervals as indicated by low gamma-ray log values. For a more complete review of the response of well logs to the presence of gas hydrate, see Collett and Lee (2012).

The analysis of log data from nine nearby wells reveals the widespread occurrence of three gas-hydrate-filled sand-rich units in the vicinity of the PBU L-pad (Collett et al., 2011; Collett et al., 2012; Lewis and Collett, 2013), which are commonly referred to as units C, D, and E in the Eileen gas hydrate trend (Figure 1a). These same units have also been shown to be gas hydrate-bearing in two previously-drilled nearby gas hydrate research wells: Northwest Eileen State #2 (Collett, 1993) and Mount Elbert-01 (Boswell et al., 2011).

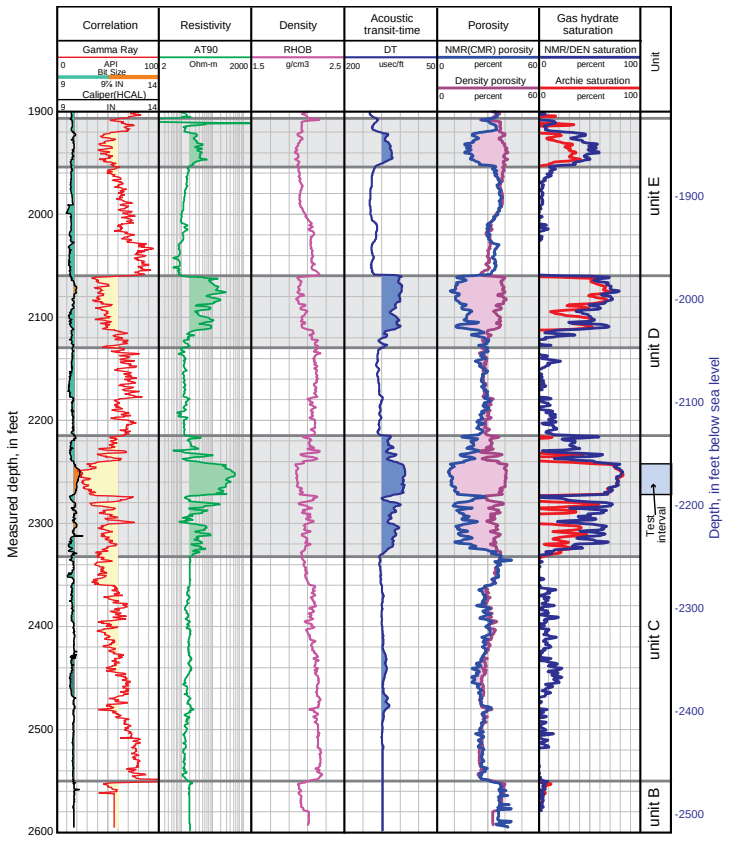

(a)

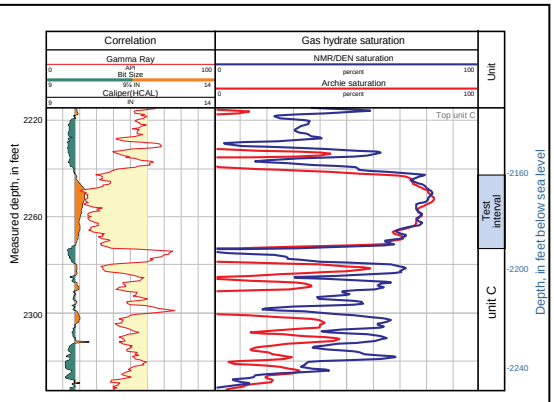

(b)

Figure 1: (a) Well log display for Iġnik Sikumi #1 test well depicting the depth of units B, C, D and E. Grey shading showing occurrence of gas hydrate within reservoir quality sands of units C, D and E. Data shown include the natural gamma ray, caliper (HCAL), electrical resistivity (AT90), bulk-density (RHOB), acoustic transit-time (DT). neutron porosity (NMR(CMR)) logs; and calculated density porosity, NMR-density derived gas hydrate saturations and Archie calculated gas hydrate saturations. (b) Well log display for Iġnik Sikumi #1 test well depicting portion of unit C. Data shown include the natural gamma ray, caliper (HCAL), calculated density porosity, NMR-density derived saturations, and Archie derived saturations. Test interval shown in blue color.

The presence of gas hydrate is inferred to occur where deep reading resistivity log (AT90) values are 20 ohm-m and greater and where the compressional-wave acoustic velocity exceeds 14 µsec/ft. Based on these criteria, three gas hydrate-bearing intervals are interpreted within the Iġnik Sikumi #1 well: 2215-2332 MD ft in unit C 2060-2130 MD ft in unit D, and 1907-1954 MD ft in unit E (Figure 1). The 30-ft-thick section within the upper part of unit C (2243-2273 MD ft) was selected for testing.

Gas hydrate saturations presented were determined using an Archie analysis of the measured resistivity log data (Archie, 1942; Lee and Collett, 2011), as well as a density and nuclear magnetic resonance (NMR) porosity log method approach (Kleinberg et al., 2005). The gas hydrate saturations estimated from the NMR and density porosities do not depend on a model or empirical parameters, so the accuracy of the estimation depends only on the accuracy of NMR and density log measurements. Therefore, it is assumed that gas hydrate saturations estimated from the NMR and density logs are the most accurate in-situ gas hydrate saturations, which have been used in this report to characterize and model the Iġnik Sikumi test results. The water saturation (S_w) is given by Archie (1942) as:

$$S_w = \left(\frac{aR_w}{\phi^m R_t} \right)^{1/n} \quad (1)$$

where n is an empirically derived parameter and is assumed to be 2.0 in this study and R_t is the formation resistivity as measured by the deep reading resistivity log (AT90) in the Iġnik Sikumi #1 well. R_w is the resistivity of the connate water, a and m are Archie constants, and ϕ is the porosity. For this study it was determined that a = 1.6 and m = 2. Resistivity of the connate pore-water determined to be approximately 1.1 ohm-m for the unit C test interval. Figures 1a and 1b show gas

hydrate saturations estimated from both the resistivity and NMR-density porosity log data, which are almost identical (averaging about 75%) within the tested interval.

We note also that S_{gh} varies between the three units: the highest values are observed in the upper C-unit, with moderate values in the D and in the lower portion of unit C, and relatively low values observed in the E unit. These variations are not assumed to be an indicator of partial or differing fill of pore space due to variations in gas availability. Instead, we infer that each unit is filled to its "petrophysically-defined capacity", with that capacity varying with grain size and clay content. Although simple production models that assume the reservoirs are petrographically-similar might suggest that the lower S_{gh} reservoirs might be more responsive to depressurization, the high S_{gh} upper C was selected as the primary test interval under the view that it is the unit with the most favorable intrinsic reservoir quality.

Volumetric analysis of the NMR log from the Iġnik Sikumi #1 well by Schoderbek et al., (2013) indicates that there is a large amount of gas hydrate in the tested portion of the C unit, along with small amounts of clay-bound water (~2%), capillary-bound water (~5%), and free-water (~4%). Estimates of permeability based on NMR-measured properties were calculated with both the SDR and Timur/Coates methods (reviewed by Collett et al., 2011). Both approaches generated permeability values greater than 1 D in the water-bearing portion of the unit C sands, but was calculated to be less than 1 mD in the hydrate-bearing portion of the upper C-unit sands.

The Schlumberger Pressure Express (XPT) tool was used to measure formation pressure and estimate fluid mobility in the unit C and D sands (Schoderbek et al., 2013). The XPT calculations indicated that mobility of the fluids in the hydrate-bearing portion of the unit C test interval are consistent with the permeabilities calculated from NMR log data, with values generally below 0.1 mD. The Schlumberger Modular Dynamic Tool (MDT) test performed in the Iġnik Sikumi #1 well did not yield any useful petrophysical data due to inability to sustain effective contact with the formation (Schoderbek et al., 2013).

Regional Reservoir Setting

In order to determine the optimal location for a test well, several geologic framework studies were performed using publically-available data from wells located on or near the PBU L-Pad (Collett et al., 2012). A total of 90 wells had sufficient gamma-ray log data through the full target interval from unit B through unit E (Figure 1a) to determine the geologic structure and the general occurrence and variation in reservoir lithology. Nine of the wells from this area have additional well log data sufficient to interpret the occurrence of gas hydrates.

A structure map on the top of unit C (Figure 2) reveals a monoclinal structure with a gentle dip of

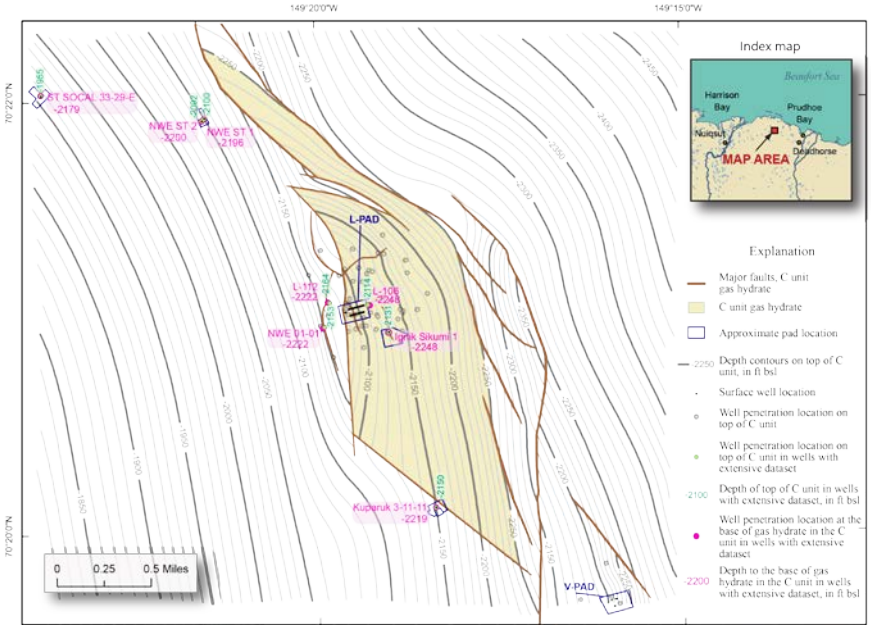

Figure 2: Structure map on top of unit C. Contour interval is 10 ft. Yellowish shading shows inferred minimal gas hydrate occurrence. BSL = below sea level.

about 3-5° to the east-northeast. This monocline is disrupted by several large arcuate, down-to-the-east, normal faults that trend roughly northwest-southeast. In both the PBU L-106 and the Iġnik Sikumi #1 well, the upper portion of the C unit is inferred to be fully saturated with gas hydrate. The lower portion of the C unit is partially filled with gas hydrate, with a gas-hydrate/water contact that occurs at approximately 2248 ft below sea level in both wells. Assuming the occurrence of gas hydrate conforms with the structure in unit C, a gas hydrate accumulation can be mapped as shown by the yellowish shading on Figure 2.

Analysis of gas hydrate to water contacts across the study area suggests that the major north-south trending faults compartmentalize the reservoir into several discrete fault blocks. Stratigraphic variation is also likely to play a role.

2012 WELL TESTING PROGRAM RESULTS

Injection Phase Interpretation

The injection phase of the Iġnik Sikumi Field Trial involved a constant pressure injection of a controlled mixture of N_2 and CO_2 with mole fractions of 0.775 and 0.225, respectively. The pressure and temperature conditions along the injection well and at the perforation were such that the injectant mixture remained in the gas phase. The injection pressure at the perforation was held nearly constant at 1420 psia, and the injection temperature was near the formation temperature.

Simulations with the STOMP-HYDT-KE simulator modeled the injection phase using a 2-dimensional 25-layered radial domain, starting at the outer radius of the well casing. Injection of the N_2-CO_2 mixture was modeled via a hydrostatic boundary condition along the well perforation zone at a constant temperature of 41.7˚F. A pressure of 1430.4 psia was assigned at a depth of 2283.0 ft MD, with vertical pressure gradient of -0.434 psia/ft. The principal objective of these simulations was model the total mass injected into the formation over the 306-hr period, which consisted of 167.3 Mscf N_2 and 48.6 Mscf CO_2. The N_2-CO_2 molar ratio in the injectant was specified via the boundary condition. A outer radial boundary at 2000 ft was set to be in equilibrium with the initial formation conditions for composition, pressure and temperature.

The geologic model for this numerical investigation was based on data collected from the test site characterization and interpretations of the research team (Schoderbek et al., 2013). The guiding principle in the development of the geologic model was to honor as much as possible the test site characterization data. The target injection horizon for the field trial was the Sagavanirktok Upper C Sand, with the injection well perforated over a 30-ft interval (2,243 to 2,273 ft MD). A computational domain was chosen with uniform vertical spacing of 2 ft that extended over a 50-ft interval (2,234 to 2,284 ft MD). Petrophysical properties for each 2-ft interval in the computational domain were varied vertically, but assumed constant radially from the Iġnik Sikumi #1 well. The computational domain extended radially from the well casing (0.375 ft) to an outer radial distance of 2000 ft. The porosity for each of the 25 strata (shown in Table 1) in the geologic model was determined by averaging over the interval the total porosity reported in log-derived reservoir properties in Table 4 of the final report (Schoderbek et al., 2013). Hydrate saturation distributions were determined by averaging over the interval the hydrate saturations reported via the NMR method reported in Figure 13 of the final report (Schoderbek et al., 2013). Effective permeability was determined by logarithmic averaging of the formation permeability determined from the XPT testing reported in Figure 17 of the final report (Schoderbek et al., 2013). Effective permeabilities are measure of the fluid mobility in the formation with the in-situ hydrate saturation. Conversion of the effective permeability to intrinsic permeability of the formation sandstone required the intrinsic porosity and hydrate saturation, according to the Civan's permeability-porosity relationship (Civan, 2001):

$$\frac{k_{eff}}{k} = \left(\frac{\phi_{eff}}{\phi}\right)\left[\frac{\phi_{eff}\left(1-\phi\right)}{\phi\left(1-\phi_{eff}\right)}\right]^{2\beta} \quad ; \varphi_{eff} = \varphi\left(1-s_h\right) \quad (2)$$

A β parameter of 1.54 in the Civan function was determined from the estimated average permeabilities in the water-bearing portion of the C sand of 1 Darcy and the hydrate-bearing uppermost portion of the C unit of 1 mD, with an average porosity of 0.4 and average hydrate saturation of 0.75. The β parameter was applied uniformly across all strata in the geologic model to

compute the intrinsic permeability distribution shown in Table 1.

Data for determining the relative permeability-saturation-capilllary (ksP) functions were collected during the characterization test at the Iġnik Sikumi #1 well. As STOMP-HYDT-KE considers the potential for three phases, four ksP functions are

Table 1: Strata Dependent Petrophysical Properties for the Geologic Model

Strata	Interval, ft MD	Porosity	Hydrate Saturation	Effective Perm., mD	Intrinsic Perm., mD	Pore Surface Area, m^2/m^3 (10^{-6})	Hydrate Surface Area, m^2/m^3 (10^{-6})
SS-1	2284-82	0.365	0.424	0.552	9.648	1.600	2.920
SS-2	2282-80	0.371	0.649	0.438	76.61	0.582	1.600
SS-3	2280-78	0.312	0.694	0.384	99.84	0.392	1.070
SS-4	2278-76	0.287	0.512	0.545	16.81	0.845	1.600
SS-5	2276-74	0.284	0.297	0.708	4.051	1.690	2.380
SS-6	2274-72	0.357	0.109	0.667	1.263	4.280	4.950
SS-7	2272-70	0.369	0.299	0.950	6.359	2.000	3.040
SS-8	2270-68	0.375	0.628	0.753	102.2	0.510	1.350
SS-9	2268-66	0.374	0.677	0.406	102.9	0.508	1.490
SS-10	2266-64	0.395	0.713	0.684	315.6	0.314	1.040
SS-11	2264-62	0.396	0.703	0.477	191.4	0.405	1.310
SS-12	2262-60	0.397	0.762	0.448	468.8	0.260	0.977
SS-13	2260-58	0.398	0.781	0.632	959.9	0.183	0.730
SS-14	2258-56	0.402	0.784	0.350	570.9	0.240	0.975
SS-15	2256-54	0.400	0.776	0.165	227.5	0.377	1.490
SS-16	2254-52	0.403	0.765	0.122	139.1	0.488	1.880
SS-17	2252-50	0.404	0.789	0.128	233.2	0.378	1.560
SS-18	2250-48	0.399	0.810	0.185	522.2	0.249	1.090
SS-19	2248-46	0.396	0.816	0.393	1224.	0.160	0.708
SS-20	2246-44	0.406	0.801	0.310	727.6	0.216	0.931
SS-21	2244-42	0.379	0.767	0.476	513.6	0.231	0.853
SS-22	2242-40	0.348	0.761	1.704	1440.	0.122	0.414
SS-23	2240-38	0.286	0.721	0.953	334.5	0.188	0.521
SS-24	2238-36	0.299	0.538	0.511	20.83	0.807	1.620
SS-25	2236-34	0.362	0.278	1.771	10.10	1.540	2.260

required: 1) saturation versus capillary pressure, 2) aqueous relative permeability versus saturation, 3) gas relative permeability versus saturation, 4) nonaqueous-liquid relative permeability versus saturation. The Iġnik Sikumi trial maintained pressure and temperature conditions that avoided the formation of a nonaqueous liquid phase. Numerical simulations conducted to provide an interpretation of the modular dynamic formation tests from the Mount Elbert-01 stratigraphic test well, Milne Point, North Slope of Alaska, yielded parameters for all but the nonaqueous-liquid relative permeability function in the C sands (Anderson et al., 2011). Functional forms and parameters for the four ksP relationships were applied uniformly across the computational domain. The saturation versus capillary pressure function used a van Genuchten (1980) form with a Webb extension (Webb, 2000) to oven-dried conditions:

$$\bar{s}_l = \frac{s_l - s_{lr}}{1 - s_{lr}} = \left[1 + \left(\alpha \beta_{gl} h_{gl}\right)^n\right]^{-m}; h_{gl} = \left(\frac{P_g - P_l}{\rho_l^* g}\right) \text{ for } h_{gl} \le h_{mp}$$

$$s_l = \frac{\log\left(\frac{h_{gl}}{h_{mp}}\right)}{\gamma} + s_{mp}; \gamma = -\frac{\log\left(\frac{h_{od}}{h_{mp}}\right)}{s_{mp}} \text{ for } h_{gl} > h_{mp}$$

$$\alpha = 10.204\, m^{-1};\ n = 4.43;\ s_{lr} = 0.28;\ m = 0.774;\ \beta_{gl} = 1.0$$

$$h_{od} = 102108.2\, m;\ h_{mp} = 0.0439\, m;\ s_{mp} = 0.984 \qquad (3)$$

The aqueous relative permeability versus saturation function used a Corey (1977) functional form:

$$k_{rl} = a(\bar{s}_l)^{\lambda};\ \bar{s}_l = \frac{s_l - s_{lr}}{1 - s_{lr}};$$
$$a = 1.0; \lambda = 4.4; s_{lr} = 0.0 \qquad (4)$$

The gas relative permeability versus saturation function used a Corey (1977) functional form:

$$k_{rg} = a(\bar{s}_g)^{\lambda};\ \bar{s}_g = \frac{s_g - s_{gr}}{1 - s_{lr}};$$
$$a = 1.0; \lambda = 2.5; s_{gr} = 0.0; s_{lr} = 0.0 \quad (5)$$

The nonaqueous-liquid relative permeability versus saturation function used a Mualem (1976) functional form:

$$k_{rn} = \sqrt{\bar{s}_n}\left[\left(1-\left(\bar{s}_t - \bar{s}_n\right)^{1/m}\right)^m - \left(1-\left(\bar{s}_t\right)^{1/m}\right)^m\right]^2 \quad (6)$$
$$\bar{s}_t = \bar{s}_n + \bar{s}_l; \bar{s}_l = \frac{s_l - s_{lr}}{1 - s_{lr}}; \bar{s}_n = \frac{s_n}{1 - s_{lr}}; m = 0.774$$

Intrinsic thermal properties of the reservoir sandstone were also not characterized either. Therefore, the grain thermal conductivity of 2.86 W/m K and grain specific heat of 700 J/kg K, used in the simulations of the Mount Elbert-01 stratigraphic test well were used uniformly across the computational domain for all strata.

The principal objective of the numerical simulations is to provide an interpretation of the data collected from the Iġnik Sikumi field trial, keeping the geologic and numerical models as simple as possible. A preliminary suite of numerical simulations was executed to calibrate the permeability parameters shown in Table 1 to the injected mass during the field trial. These simulations included both isotropic and anisotropic ratios of vertical to horizontal intrinsic permeability. The results from these simulations indicated good agreement between the simulations and field-trial data occurred using a vertical to horizontal anisotropy ratio of 0.1 and by scaling the scaling the intrinsic permeabilities by a factor of 1.5 from those shown in Table 1. A suite of injection simulations were executed that differed in the kinetic exchange rate constant, kinetic hydrate dissociation constant, kinetic hydrate formation constant, and ice pore clogging model. A typical plot of cumulative injected mass versus time is shown in Figure 3, with the total inject gas being 232.4 Mscf, compared with the field value of 215.9 Mscf. During the injection phase, there were only minor differences in the injected mass across the suite of simulations with varying kinetic parameters and ice pore clogging model.

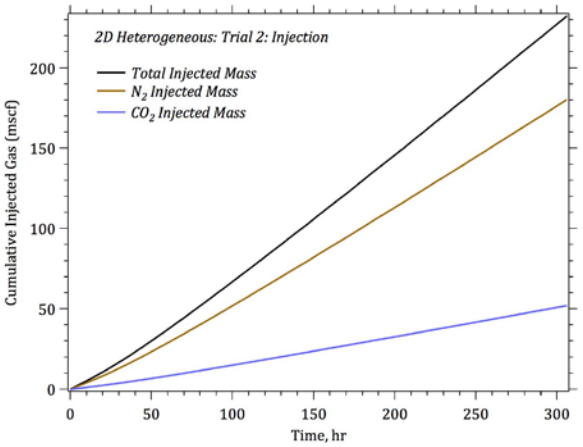

Figure 3: Cumulative injected N_2 and CO_2 mass during the Injection Phase for Simulation #2.

The multifluid flow, phase transformation, and heat transfer processes occurring in the hydrate reservoir with the injection of N_2 and CO_2 are complex and strongly coupled. The state of the hydrate and gas saturations at the end of the injection phase (i.e., after 306 h) is shown in Figures 4 and 5, respectively. The hydrate saturation vertical profile at the 20-m radial distance provides an indication of the initial hydrate saturation distribution via the strata. During the injection phase both primary hydrate dissociation and secondary hydrate formation occurred. The gas saturation profile is non-uniform due to the initial heterogeneities in the effective permeabilities and the changes in the hydrate saturation. Maximum migration of the gas into the reservoir is roughly 7 m from the center of the well.

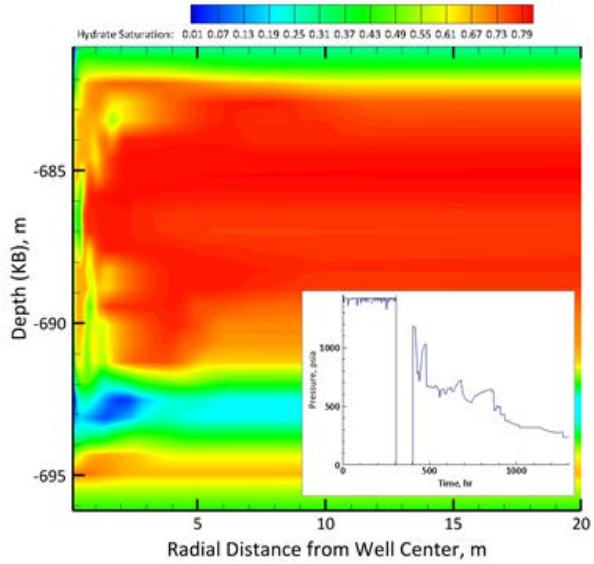

Figure 4: Hydrate saturation at the end of the injection phase for Simulation #2

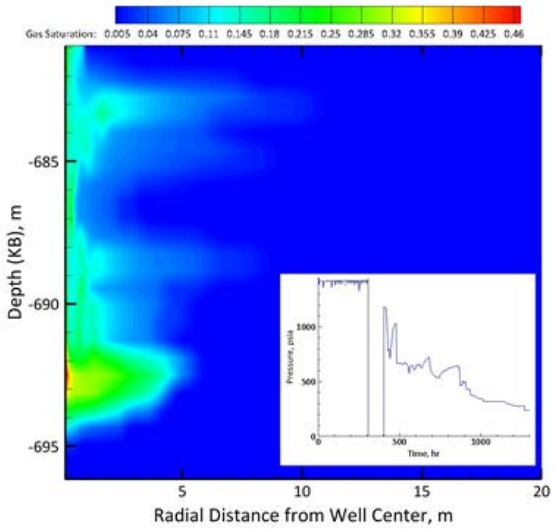

Figure 5: Gas saturation at the end of the injection phase for Simulation #2

The state of the temperature at the end of the injection phase (i.e., after 306 h) is shown in Figure 6. Near freezing conditions are predicted to occur in those regions where hydrate dissociation occurred and elevated temperatures are noted where the secondary hydrate formed, primarily in regions of lower initial hydrate saturations. It should be noted that the freezing temperature regions are not adjacent to the well casing, where the temperature of the injected gases helps to maintain the initial reservoir conditions. The region of increased gas pressure extends well beyond the gas saturation plume, which is typical for the injection of gases into saline formations.

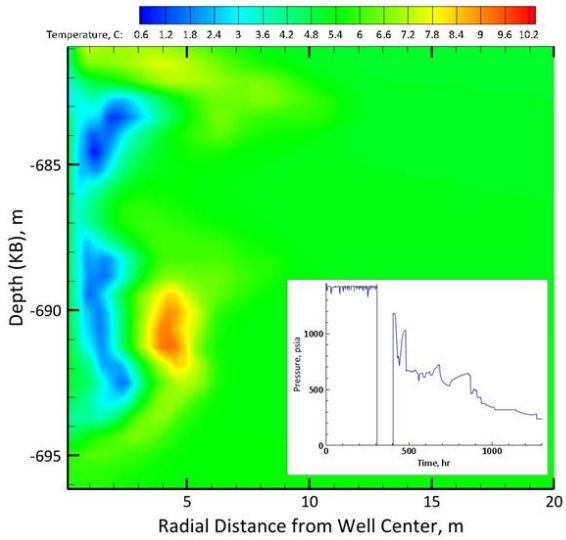

Figure 6: Temperature at the end of the injection phase for Simulation #2

The state of the N_2, CO_2, and CH_4 hydrate mole fraction of formers (i.e., ignoring hydrate water) at the end of the injection phase (i.e., after 306 h) is shown in Figure 7 a, b, and c, respectively. The exchange of guest molecules is primarily controlled by the concentration of injected N_2 and CO_2, yielding hydrate with higher concentrations of N_2. Deeper in the reservoir the hydrate is primarily a binary N_2-CH_4 form, with the CO_2 being depleted in the region nearer to the well. Adjacent to the well are regions of CH_4 free hydrate that form with exposure of the hydrate to freshly injected N_2 and CO_2, as shown in Figure 7c. Changes in the hydrate composition yield changes in the hydrate equilibrium pressure, with higher equilibrium pressures occurring in regions of higher temperatures and increased hydrate concentrations of N_2 and CO_2.

A suite of simulations were conducted for all three phases of the Iġnik Sikumi Field Trial. Six simulations from the suite are reported here, and principally vary in the guest-molecule exchange rate and the ice pore plugging model. The kinetic formation/dissociation constant used in Simulations #2 and #2c were roughly 10 times those used by Sun et al. (2005). The use of a bound-water saturation of 0.2 limits the formation and the rate of formation of hydrates. Injection of the N_2-CO_2 into the reservoir creates gas saturation around the injection well and yields a positive driving force for the exchange of N_2 and CO_2 with CH_4 in the hydrate. The rate of exchange is controlled by the kinetic exchange rate parameter and the difference in former vapor pressures and hydrate equilibrium partial pressures. As N_2 and CO_2 exchange with the CH_4 in the hydrate the hydrate composition shifts as does the hydrate equilibrium pressure, density, and enthalpy. The injection rates force the gas mixture deeper into the reservoir, transporting unexchanged N_2 and CO_2, and exchanged CH_4 away from the well.

Gas migration is controlled by the heterogeneity in the effective permeability of the strata and the heterogeneity that develops as hydrate dissociates and forms in response to the gas mixture injection. When the kinetic exchange rate constant is increased to 1.0×10^{-3} kmol/m^3 a greater percentage of the injected N_2 and CO_2 becomes incorporated into hydrate rather than remaining in the mobile phases (i.e., aqueous and gas). An interesting result from these simulations is that there is a net

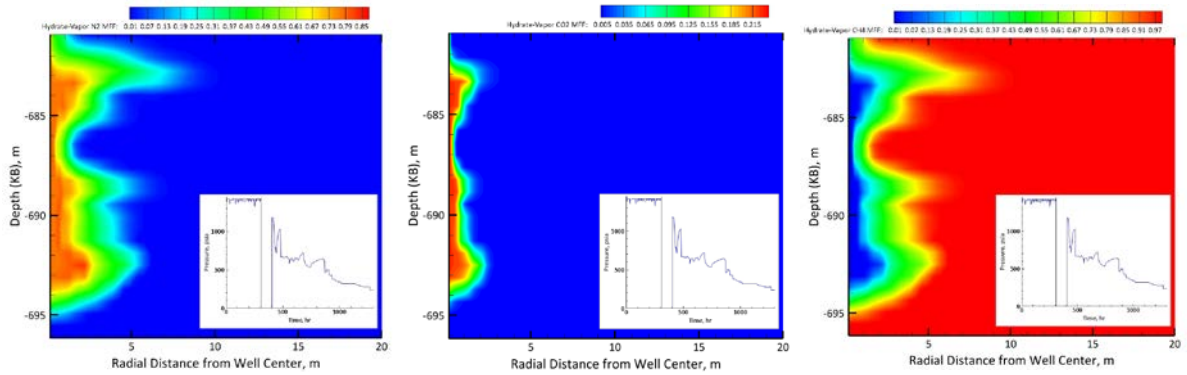

Figure 7: Hydrate (a) N_2, (b) CO_2, and (c) CH_4 mole fractions at the end of the injection phase for Simulation #2

increase in the hydrate mass, primarily due to the increase in hydrate density with the alteration in hydrate composition. The CH_4 rich hydrate has a density of around 915 kg/m^3, whereas the N_2 and CO_2 rich hydrate has a density of around 1080 kg/m^3. This shift in hydrate density alters the effective molar exchange ratio of guest-molecules to be more than 1 to 1.

Mix3HydrateResSim: Similar methods to the STOMP-HYDT-KE simulations were performed using Mix3 HRS. Composition was controlled with an average injection ratio of 77.5/22.5 N_2/CO_2 during the injection period. During the injection, the well is modeled as a fixed-condition boundary with a gas phase (23% CO_2+ 77% N_2) at 9.75 MPa and 5°C. In order to match the field test injected gas flow rates, the permeability value and the relative permeability function parameters of the hydrate layer are varied. The permeability of the hydrate layer is 40 mD and the relative permeability parameters are given in Table 3 for the best match. The permeability at the interface between two grid blocks is evaluated as the harmonic weighted averaging of permeabilities of individual blocks. Harmonic weighting uses both upstream and downstream parameters and as the flow is from the injection well into the reservoir it is more appropriate to use harmonic weighting than upstream weighting.

In the field test while maintaining a constant 9.75 MPa bottom hole pressure, the injection rate began to decrease during the first days of injection. However, around 50 hrs, the injection rate leveled off and then began to steadily increase through the remainder of the injection phase. In model the injection rate began to decrease during the first few hours. This can be due to the secondary hydrate formation which caused to decrease the permeability of the system but the rates leveled off immediately after few hours. The calculation of relative permeability of the phase is considered to be function of the saturation of the respective phase but it is not a direct function of the hydrate saturation. The hydrate formation and dissociation might have more effect on the permeability of the gas phase in the reservoir which caused the discrepancy in the flow rates from the experimental data. The final state is then used as the initial state for the production simulations. The cumulative standard volumes of CO_2 and N_2 injected into the system are shown in Figure 8.

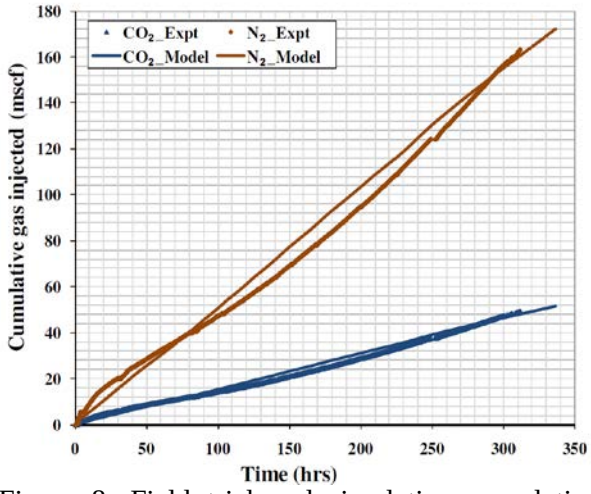

Figure 8: Field trial and simulation cumulative injected gas using Mix3HRS

After the 14-day injection period, the well was shut-in while operations were shifted to production mode. The shut-in period lasted about 4.5 days. As expected, the bottom hole pressure began to fall off after injection. Over the post-injection period, down hole pressure went from an initial pressure of 9.1 MPa to 8.27 MPa. (Schoderbek, 2012). This period is modeled by changing the

injection blocks permeability to be zero. The pressure of the blocks next to the well bore in the hydrate layers during the simulation are shown in Figure 9 and are compared with the actual bottom hole pressure.

The pressure in the first blocks of the bottom three hydrates layers followed the actual bottom hole pressure profile, but there is a small increase in the pressure observed in the top three layers as the top and third hydrate layers are saturated with hydrate and there is no flow observed in those layers. These highly saturated layers caused worm holes in the reservoir and produced solid hydrate during production.

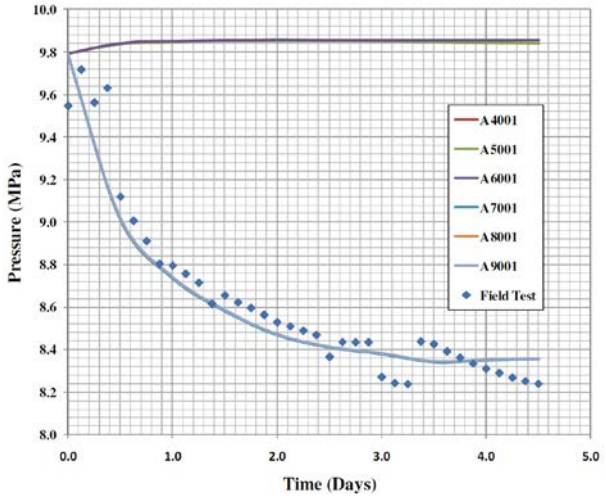

Figure 9: Field trial and simulation cumulative injected gas using Mix3HRS

Flow-back Phase Interpretation

STOMP: As the STOMP-HYDT-KE simulator is inherently kinetic the 92.5-hr period between the injection and flow-back phases of the field trial were simulated using zero-flux boundary conditions at the well perforation zone. The outer radial boundary condition was maintained at the initial conditions. During this soak phase, guest-molecule exchange continued and redistribution of phases occurred. The soak phase simulations were initiated with the final time conditions from the simulations of the injection phase. Likewise, the flow-back phase simulations were initiated with the final time conditions from the simulation of the soak phase.

The flow-back phase of the Iğnik Sikumi Field Trial involved 1 unassisted flow-back period, followed by 3 jet-pump flow-back periods. Between each flow-back period was a shut-in period with a pressure recovery. The shut-in periods were modeled, using zero-flux boundary conditions at the well casing. The outer radial boundary condition was maintained at the initial conditions throughout the flow-back phase simulations. The metrics of interest during the flow-back phase simulations were the produced gas and water from the field trial data, and the ratios of produced N_2, CO_2 and CH_4.

A suite of simulations were conducted for the flow-back phase. Simulation #2 used guest-molecule exchange rates that were in agreement with numerical simulations of kinetic exchange experiments conducted at the Korea Institute of Geoscience and Mineral Resources. Simulation #6 used an exchange rate 10 times higher, and Simulation #10 used an exchange rate 10 times lower than that of Simulation #2. The total cumulative produced gas and water (i.e., aqueous) for Simulation #10 are shown in Figure 10. The produced gas included N_2, CO_2, and CH_4 dissolved in the aqueous phase. For reference the field trial data (Schoderbek et al., 2013) are shown in the plot. There are two stark differences between the simulation results shown in Figure 10 compared with the field trial data. The first is that the sharp increase in produced gas during the second jet-pump flow-back period (i.e., 269-333 hr) is not captured at all in the simulation results. The second difference occurs during the third jet-pump flow-back period (i.e., 448-898 hr), where the produced aqueous rate from the simulation matches that of the field-trial data, but the produced gas rate from the simulation is much lower than that of the field-trial. There is also little difference between the produced gas for simulations for the three different guest-molecule exchange rates.

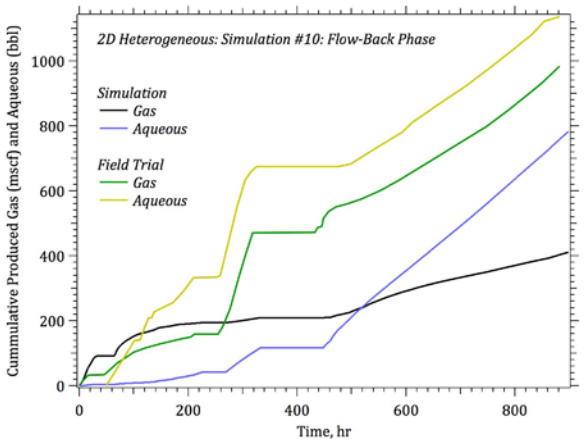

Figure 10: Produced gas and water for Simulation #10 ($K_e = 10^{-5}$ *kmol/m^3 s)*

Well pressures during the third jet-pump flow-back period fall below the equilibrium pressure of the mixed hydrate, which should lead to hydrate dissociation and cooling. The numerical simulations all predict ice formation in the region around the well, which obstructs gas flow to the well. The ice accumulation around the perforation zone of the well strongly inhibits gas flow into the production well. To investigate the impact of ice formation, the three flow-back phase simulations were repeated, but without the formation of ice having any impact on the effective permeability. The total cumulative produced gas and water (i.e., aqueous) for Simulation #10c are shown in Figure 11 as solid lines. These plots show the impact of ice plugging on the gas flow. Without ice plugging the gas flow rates trend more toward those observed in the field trial.

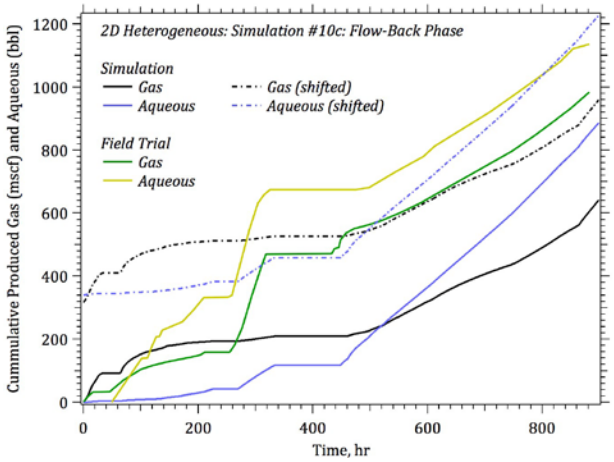

Figure 11: Produced gas and water for Simulation #10c ($K_e = 10^{-5}$ *kmol/m^3 s)*

The sharp increase in produced gas and water observed in the field trial during the second jet-pump flow-back period (i.e., 269-333 h) was associated with sand production, with an average of 2.6% volume of sand (Schoderbek et al. 2013). Plots of productivity versus time during this period show a dramatic increase in flow potential, which was attributed to a dramatic increase in permeability. The combined observations of sharp increases in gas production, produced sand, and permeability, suggest that hydrate was being pulled into the wellbore and dissociating in the wellbore. If the STOMP-HYDT-KE cumulative gas and water production plots are adjusted by the amounts of observed produced gas (i.e., 317.7 Mscf) and water (i.e., 341.2 bbl), then a comparison of trends in production during the third jet-pump flow-back period between the simulations and observations can be more easily made. Adjusted plots of produced gas and water from the Simulation #10c are shown in Figure 12 as broken lines. With these adjustments the simulated trends show good agreement with the field trial observations.

An interesting observation from the Iġnik Sikumi Field Trial is that the ratio of N_2 and CO_2 gases recovered was not the same as injected. This indicates that partitioning of the gases is occurring, either via incorporation into hydrate or via dissolution in the aqueous phase. Plots of the recovered gases in terms of fraction of injected gas are shown in Figure 12 for Simulation #10c. These plots more clearly show the impact of the guest molecule exchange rate parameter. The slower rate parameter of Simulation #10c shows closer agreement with the field trial observations, but the simulation results over predict the amount of recovered N_2 and CO_2 components.

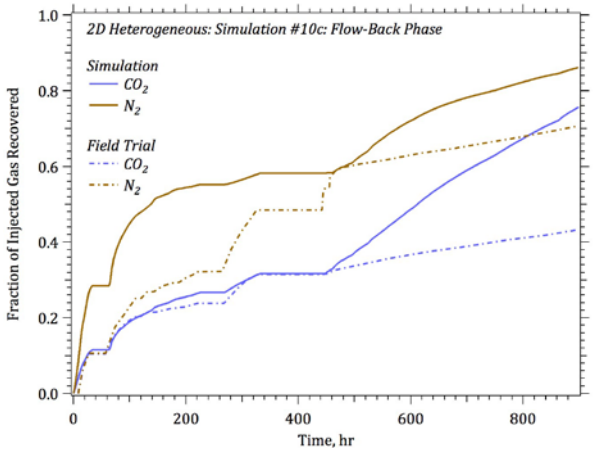

Figure 12: Produced gas and water for Simulation #10c ($K_e = 10^{-5}$ *kmol/m^3 s)*

The state of the formation at the end of the flow-back phase shows combinations of dissociation and guest-molecule exchange processes. Within the perforation zone hydrate dissociation has occurred, but only a few meters into reservoir for Simulation #10c, which does not consider permeability reduce with ice formation. The gas saturation additional appears in the region between the dissociation front and well casing within the perforation zone, providing a pathway for gas flow from the dissociating hydrate and production well for Simulation #10c. Nitrogen which has been incorporated into hydrate and remains in hydrate form, only occurs above and below the perforation zone for Simulation #10c. The N_2 that was

incorporated into hydrate within the perforation zone, has vanished with the dissociation of the hydrate. The hydrate CO_2 distribution, however, is in contrast to that of N_2, occurring primarily within the perforation zone, just on the fringe of the hydrate region. This simulation result is not completely understood, but could be due to dissolved CO_2 forming hydrate as water flows into the colder region at the hydrate dissociation front.

Mix3HydrateResSim*:* During the production phase of the field test, sand production was observed and it is estimated that about 67 barrels of sand is produced (Schoderbek et al., 2013). In the original code the movement of solid particles is not considered. Therefore the code was also modified to account for the sand production and potential solid hydrate production along with sand that could dissociate subsequently in the well bore which causes worm holes (*x*) in the grid block with high permeability. The concept that each grid block consists of two parts, one with the original permeability and the other with a high permeability presented by (Kurihara et al., 2011) is introduced to represent the increase and decrease in the effective permeability for each grid block. The production phase is modeled by maintaining a fixed-state boundary as an aqueous phase at the bottom-hole pressure. The permeability at the interface between two grid blocks is evaluated as an upstream weighted averaging of permeabilities of individual blocks as now the flow is from the reservoir to the production well and upstream weighting uses only upstream parameters and numerically much more robust than the harmonic weighting. The CH_4 gas production is matched by varying the value of *x*. The history matching of cumulative amount of CH_4 gas is shown in Figure 13.

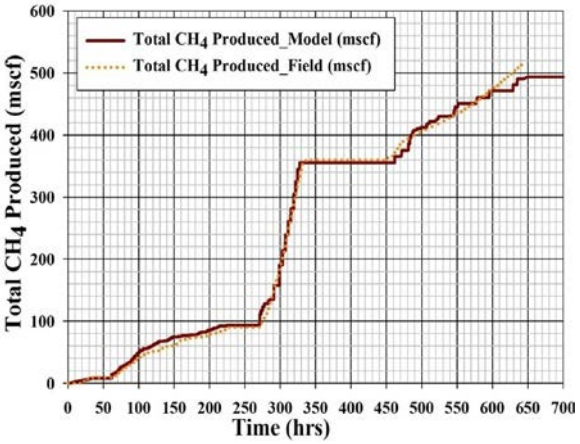

Figure 13: Cumulative volume of CH_4 gas during the production period from Mix3HRS.

The history match for cumulative amounts of CO_2 and N_2 are given in Figure 14 (a) and (b). It was found that the N_2 production values from the model are lower than the actual data, and CO_2 values match at end of the high flow period and exceed the actual field data for the last flow period. The amounts of gas present in the well bore before the production were accounted for by using the Peng Robinson equation of state and were calculated to be about 9.2 mscf of N_2 and 2.6 mscf of CO_2 present in the well bore. The prediction of lower amounts of N_2 gas through the simulation could be due to the assumption that the hydrate is considered to be a mixed hydrate in the reservoir. But there could be formation of simple hydrates and N_2 hydrate being unstable at the prevailing conditions more N_2 gas is produced than predicted while CO_2 hydrate is stable at low pressure and there is a lower amount of CO_2 gas observed during last phase in field data.

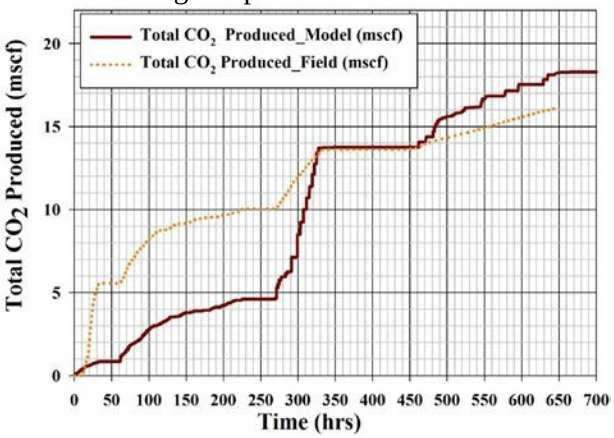

(a)

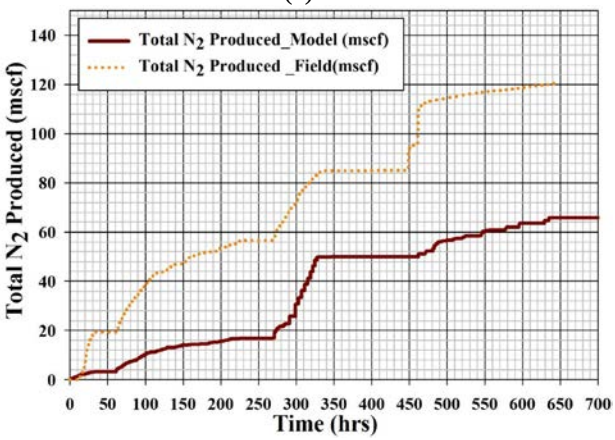

(b)

Figure 14: Cumulative volumes of CO_2 (a) and N_2 (b) gas during the production period from Mix3HRS.

Over the course of the production test approximately 70% of nitrogen and 40% of carbon dioxide was recovered. In contrast, the Mix3HRS model results in N_2 and CO_2 recovery of 39% and 36% respectively.

DISCUSSION

There are two key differences in the approaches taken in this paper using STOMP-HYDT-KE and Mix3HydrateResSim: the use of kinetic exchange rates by STOMP-HYDT-KE and the simulation of sand production and its effects on gas production. It is clear from the kinetic analysis that gas exchange rates in the Iġnik Sikumi field trial are slower than that as seen in laboratory experiments. This may be on the order of 10 times slower and could be due to a number of reasons including ice formation, CO_2 hydrate shell formation, or other undetermined mechanisms that slow gas exchange. Additionally, it is clear that the ratio of gas recovered as seen in the field trial is better reproduced using some form of slow kinetic exchange rates as opposed to an equilibrium assumption. However, the full field trial cannot be explained without consideration of the production of sand and possibly solid hydrate and the effect of sand production on gas production. A combination of the two approaches presented in this paper must be considered in order to account for all of the complex results seen in the Iġnik Sikumi field trial.

SUMMARY AND CONCLUSIONS

The Iġnik Sikumi Gas Hydrate CO_2-CH_4 Exchange Field Trial was conducted to provide insight into basic scientific and engineering issues related to the potential for future application of the technology for synergistic gas production and CO_2 sequestration in gas hydrate reservoirs. In accordance with the objectives and the logistics of Alaska North Slope operations, the field trial was conducted as a single-well "huff and puff" that featured the injection of mixed CO_2+N_2 gas followed by flowback enabled via staged depressurization.

The commercial viability of exchange technology will be strongly driven by the potential CH_4 production rates. Reservoir engineering and field-scale trials need to be undertaken to fully appraise the nature of chemical exchange across a range of heterogeneous natural reservoir systems. Given the results of this initial field trial as outlined below, additional field tests, laboratory, and modeling studies will be required to refine production strategies (well configuration, injection method, injection gas chemistry, etc.) that will maximize production rate, reservoir deliverability, and reservoir stability.

Key Findings and Observations

1. The Iġnik Sikumi #1 logging program confirmed the occurrence of multiple gas-hydrate-bearing sand reservoirs within "Eileen" gas hydrate trend in the western portions of the Prudhoe Bay Unit in accord with earlier interpretations (Collett et al., 2011).

2. The reaction of the well to any cessation of active energy input was rapid re-stabilization of gas hydrate within the well-bore and the formation. In addition, the reservoir was highly responsive to even modest changes in bottom-hole pressure. These phenomena confirm that gas hydrate production via depressurization is readily controlled and not prone to "chain reaction" or otherwise becoming uncontrollable.

3. Well log data as well as reservoir response to injection supports the occurrence of free water within native methane hydrate formations. Production concepts featuring injection must account for its presence. Further, future laboratory and numerical modeling studies of chemical exchange should address this situation.

3. Injectivity in the presence of high hydrate saturations as well as free water will be slow, but can be achieved with proper mixes of CO_2 with other components (such as, but not necessarily optimally, nitrogen) that can inhibit hydrate formation.

4. Based on the preferential retention of CO_2 in the reservoir compared to N_2, it was observed that CO_2 was successfully sequestered relative to N_2 through either exchange with CH_4 in the hydrate phase or through the partitioning of CO_2 from N_2 during new hydrate formation.

5. Gas hydrate production in general will likely lead to the need to deal with water and sand production, and both research boreholes and commercial boreholes will need suitably designed gravel packs, screens and pumps. Wellbores must also provide means to deliver heat/inhibitors close

to the producing formation to prevent hydrate formation in the wellbore during inevitable interventions.

6. Having demonstrated injectivity and production, this test enables scientific consideration of progression to the next logical phase in exchange evaluation, a two-well test (one injector and one producer) with design of enabling exchange in injector region and potentially additional depressurization/thermal stimulation in the producer region.

7. Managing well production via control of downhole temperature above the freezing point of water was demonstrated quite readily. Using temperature as the control might provide options for lower pressure drawdowns and higher rates than prior modeling which focused on setting downhole pressure had indicated.

8. We expect ongoing evaluation of the test data to develop further, and more specific, scientific learnings from the test, including observations of the thermal capacity of permafrost, the thermal response (and the parameters related to ice formation) of hydrate reservoirs to dissociation, the range of potential production rates achievable through mixed gas injection, the fate of injected gases, including CO_2, and many others

Remaining Challenges

Basic science: At present, much of what is known regarding the behavior of CH_4 hydrates in the presence of CO_2 is based on experimental studies using bulk hydrates or water-free porous-media settings that likely behave very different from natural reservoir settings. For example, it is known that the basic equilibrium conditions differ in a complex manner between bulk and porous media settings. Further, the basics of the thermodynamic behavior of complex systems including multiple gases is very poorly known, greatly restricting the ability to model fundamental reactions of interpret gathered field data. Natural gas hydrate formations are of generally high intrinsic permeability, however, when gas hydrate saturations are high (50% +) permeability is typically very low (< 0.2 md). More importantly, however, the ability to inject CO_2 into free-water-bearing reservoirs is challenged significantly by the potential for injectivity loss as the injected CO_2 reacts with free water to CO_2-hydrate prior to any interaction with the native methane hydrate. While mixed gases appear necessary to enable injection, there remains limited experimental and modeling information available to support design of appropriate mixed and evaluation of phenomena resulting from mixed gas injection.

Complex Thermodynamics: While the ability to predict the equilibrium thermodynamics of various mixed gas systems is well advanced, very little is known regarding either the kinetics of mixed gas hydrate formation/dissociation or the nature of any porous media affects. These issues are further complicated by the non-stoichiometric nature of gas hydrates, which allows virtually any combination of guest molecules to contribute to gas hydrate formation. In addition to thermodynamic stability, issue of gas solubility in formation waters, variable formation water chemistry, etc. must also be considered. At present, numerical models capable of two-gas systems (CO_2, CH_4) are increasingly advanced; however, modeling capabilities for three-gas systems remain in an early stage of development (Garapatti et al., 2011).

Physical Process: The means by which exchange of guest gas molecules occurs remains unresolved. The University of Bergen/ConocoPhillips research program appeared to suggest that no wholesale dissociation and lattice reformation occurs (Stevens et al., 2008), and it seems plausible that various degrees of partial cage destruction or significant lattice distortion occurs. However, total dissociation and reformation at very short time-scales cannot be ruled out.

Recovery efficiency: Whereas depressurization will theoretically dissociate 95% or more of the gas hydrate within the area of influence of a production well, CO_2 will only replace CH_4 in the larger cages of the clathrate structure, yielding a theoretical limit for exchange efficiency at 64% (Lee et al., 2003). Further studies have shown that mixed gas injection (i.e., CO_2 + N_2) can boost recovery to 85% (Park et al., 2006) as the second gas achieves some displacement from the smaller sI cages.

ACKNOWLEDGMENTS

B.A. performed this work under contract DE-FE0004000, Subtask 4000.4.605.261.001 in support of the National Energy Technology

Laboratory's Office of Research and Development.

DISCLAIMER

Any use of trade, product, or firm names is for descriptive purposes only and does not imply endorsement by the U.S. Government.

REFERENCES

Anderson, B.J., Hancock, S.H., Wilson, S.J., Enger, C.S., Collett, T.S., Boswell, R.M., Hunter, R.B., 2011, Formation pressure testing at the Mount Elbert Gas Hydrate Stratigraphic Test Well, Alaska North Slope: Operational summary, history matching, and interpretations. Marine and Petroleum Geology 28(2), pg 478-492.

Archie, G.E., 1942, The Electrical Resistivity Log as an Aid in Determining Some Reservoir Characteristic: Journal of Petroleum Technology, v. 5, p. 1-8.

Baldwin, B., Stevens, J., Howard, J., Graue, A., Kvamme, B., Aspenes, E., Ersland, G., Husebo, J., Zornes, D., 2009. Using magnetic resonance imaging to monitor CH_4 hydrate formation and spontaneous conversion of CH_4 hydrate to CO_2 hydrate in porous media; Magnetic Resonance Imaging 27, 720-726.

Boswell, R.., Collett, T., Anderson, B., and Hunter, R., eds., 2011, Scientific Results of the Mount Elbert Gas Hydrate Stratigraphic Test Well, Alaska North Slope: Journal of Marine and Petroleum Geology, v. 28, no. 2, 595 p.

Civan, F. 2001, Scale effect on porosity and permeability: Kinetics, model, and correlation. AIChE J., 47: 271–287.

Collett, T.S., 1993, Natural Gas Hydrates of the Prudhoe Bay and Kuparuk River area, North Slope, Alaska: American Association of Petroleum Geologists Bulletin, v. 77, no. 5, p. 793-812.

Collett, T. S., A. H. Johnson, C. C. Knapp, and R. Boswell, 2009, Natural Gas Hydrates: A Review, in T. Collett, A. Johnson, C. Knapp, and R. Boswell, eds., Natural gas hydrates—Energy resource potential and associated geologic hazards: AAPG Memoir 89, p. 146– 219.

Collett, T.S., Boswell, R., Lee, M.W., Anderson, B.J., Rose, K., and Lewis, K.A., 2012, Evaluation of long-term gas-hydrate-production testing locations on the Alaska North Slope: Society of Petroleum Engineers, Reservoir Evaluation and Engineering, v. 15, no. 2, p. 243-264.

Collett, T.S., and Lee, M.W., 2012, Well log characterization of natural gas hydrates: Petrophysics, v. 53, no. 5 (October 2012), p. 348-367.

Collett, T., Lee, M., Agena, W., Miller, J., Lewis, K., Zyrianova, M., Boswell, R., and Inks, T., 2011, Permafrost-associated natural gas hydrate occurrences on the Alaska North Slope: Journal of Marine and Petroleum Geology, v. 28, no. 2, p. 279-294.

Corey, A. T., 1977, Mechanics of Heterogeneous Fluids in Porous Media. Water Resources Publications, Fort Collins , Colorado , 259 pp.

Garapati, N., Velaga, S., Anderson, B., 2011. Development of thermodynamic framework for the simulation of mixed gas hydrates; formation, dissociation and CO_2-CH_4 exchange. ICGH-2011, 7pp.

van Genuchten, M.Th., 1980, "A closed-form equation for predicting the hydraulic conductivity of unsaturated soils". Soil Science Society of America Journal 44 (5): 892–898.

Graue, A., Kvamme, B., Baldwin, B., Stevens, J., Howard, J. J., Aspenes, E., ... & Zornes, D. (2008). MRI visualization of spontaneous methane production from hydrates in sandstone core plugs when exposed to CO_2. SPE Journal, 13(02), 146-152.

Hester, K., Stevens, J., Howard, J., 2011. Composition studies to determine rate and extent of CO_2 exchange in a hydrate-bearing core. ICGH-2011. 5 pp.

Kleinberg, R.L., Flaum, C., and Collett, T.S., 2005, Magnetic Resonance Log of Mallik 5L 38: Hydrate Saturation, Growth habit, and Relative Permeability, in S.R. Dallimore and T.S. Collett (eds.), Scientific Results from the Mallik 2002 Gas Hydrate Production Research Well, Mackenzie Delta, Northwest Territories: Geological Survey of Canada Bulletin 585, 15 p.

Lee, H., Seo, Y., Seo, Y., Moudrakovski, I., Ripmeester, J., 2003. Recovering Methane from Solid Methane Hydrate with Carbon Dioxide. Angewandte Chemie-International Edition. 42(41):5048-5051.

Kurihara, M., Funatsu, K., Ouchi, H., Sato, A., Masuda, Y., Yamamoto, K., et al., "Analysis of 2007/2008 JOGMEC/NRCan/Aurora Mallik gas hydrate production test through numerical simulation," In Proceedings of the 7th International Conference on Gas Hydrates. Edinburgh, Scotland, United Kingdom, 2011.

Lee, M.W., and Collett, T.S., 2011, In-situ Gas Hydrate saturation Estimated from Various Well Logs at the Mount Elbert Gas Hydrate Stratigraphic Test Well, Alaska North Slope: Journal of Marine and Petroleum Geology, v. 28, no. 2, p. 439-449.

Lewis, K.A., and Collett, T.S., 2013, Brookian sequence well log correlation sections and occurrence of gas hydrates, north-central North Slope, Alaska: U.S. Geological Survey Scientific Investigations Report 2013–5050, 23 p., http://pubs.usgs.gov/sir/2013/5050/.

McGrail BP, HT Schaef, MD White, T Zhu, AS Kulkarni, RB Hunter, SL Patil, AT Owen, and PF Martin. 2007. Using Carbon Dioxide to Enhance Recovery of Methane from Gas Hydrate Reservoirs: Final Summary Report. PNNL-17035

Mualem, Y., 1976, A new model for predicting the hydraulic conductivity of unsaturated porous media, Water Resour. Res., 12(3), 513–522

Park, Y., Kim, D., Lee, J., Huh, D., Park, K., Lee, J., Lee, H., 2006. Sequestering carbon dioxide into complex structures of naturally occurring gas hydrates. PNAS 103-34. pp. 12690-12694.

Schoderbek, David, Martin, Kenneth, Howard, James, Silpngarmlert, Suntichai, and Hester, Keith, 2012, North Slope hydrate field trial: CO2/CH4 exchange: Proceedings Arctic Technology Conference, December 3-5, 2012, Houston, Texas, 17 p.

Schoderbek, David, Farrel, Helen, Hester, Keith, Howard, James, Raterman, Kevin, Silpngarmlert, Suntichai, Martin, Kenneth Loyd, Smith, Bruce, and Klein, P., 2013, ConocoPhillips Gas Hydrate Production Test Final Technical Report, Prepared by ConocoPhillips Company for the United States Department of Energy, National Energy Technology Laboratory, 204 p. http://www.netl.doe.gov/File%20Library/Research/Oil-Gas/methane%20hydrates/nt0006553-final-report-hydrates.pdf

Stevens, J., Husebo, J., Ersland, G., Baldwin, B., Graue, A., Howard, J., 2008. Experimental hydrate formation and gas production scenarios based on CO_2 sequestration. Proceedings, 6th International Conference on Gas Hydrates 2008.

Webb, S. W., 2000, A simple extension of two-phase characteristic curves to include the dry region, Water Resour. Res., 36(6), 1425–1430